Cardiovascular Research (2016) **109**, 397–408
doi:10.1093/cvr/cvv260

Cardiomyocyte exosomes regulate glycolytic flux in endothelium by direct transfer of GLUT transporters and glycolytic enzymes

Nahuel A. Garcia[1], Javier Moncayo-Arlandi[2], Pilar Sepulveda[1,3]*, and Antonio Diez-Juan[4,5]*

[1]Mixt Unit for Cardiovascular Repair, Instituto de Investigación Sanitaria La Fe-Centro de Investigación Príncipe Felipe, Valencia, Spain; [2]Cardiovascular Genetics Center, Institut d'Investigació Biomèdica de Girona, Girona, Spain; [3]Regenerative Medicine and Heart Transplantation Unit, Instituto de Investigación Sanitaria La Fe, Adva. Fernando Abril Martorell 106, 46026 Valencia, Spain; [4]Fundación IVI/INCLIVA, Valencia, Spain; and [5]IGENOMICS, Calle Catedrático Agustín Escardino 9, Paterna, Valencia 46980, Spain

Received 27 April 2015; revised 5 October 2015; accepted 10 November 2015; online publish-ahead-of-print 25 November 2015

Time for primary review: 33 days

Aims Cardiomyocytes (CMs) and endothelial cells (ECs) have an intimate anatomical relationship, which is essential for maintaining the metabolic requirements of the heart. Little is known about the mechanisms that regulate nutrient flow from ECs to associated CMs, especially in situations of acute stress when local active processes are required to regulate endothelial transport. We examined whether CM-derived exosomes can modulate glucose transport and metabolism in ECs.

Methods and results In conditions of glucose deprivation, CMs increase the synthesis and secretion of exosomes. These exosomes are loaded with functional glucose transporters and glycolytic enzymes, which are internalized by ECs, leading to increased glucose uptake, glycolytic activity, and pyruvate production in recipient cells.

Conclusion These findings establish CM-derived exosomes as key components of the cardio-endothelial communication system which, through intercellular protein complementation, would allow a rapid response from ECs to increase glucose transport and a putative uptake of metabolic fuels from blood to CMs. This CM–EC protein complementation process might have implications for metabolic regulation in health and disease.

Keywords Cardiomyocyte • Exosomes • Endothelium • Protein complementation • Glycolysis

1. Introduction

Heart capillaries possess continuous endothelium adjacent to cardiomyocytes (CMs). Although the bulk of cardiac tissue mass is represented by CMs, the number of myocardial endothelial cells (ECs) exceeds CMs by 3 : 1.[1] Close contact between capillary ECs and CMs guarantees an optimal diffusion of oxygen and nutrients between blood and myocardium, and allows reciprocal signalling mechanisms to engage. Numerous studies have shown that ECs affect cardiac performance[2,3] and, reciprocally, CMs also modulate EC function.[4] Therefore, a direct path of communication exists between the two. However, whether this pathway functions in acute situations, which would be crucial for the control of metabolic demand of individual CMs, is unknown. The physical proximity of ECs to CMs suggests the possibility of transfer of metabolic information from CMs to ECs, according to local conditions, which would induce an immediate response from the adjacent ECs. Ideally, this response would be rapid and preferably would occur without gene transcription/protein synthesis.

Intercellular transfer of exosomes is a well-established mechanism allowing cell-to-cell communication. Exosomes are released into the extracellular milieu by a wide range of cell types, including CMs.[5] Exosomes contain a variety of biological materials comprising mRNAs, mirRNAs, proteins, and lipids, which can directly stimulate target cells or transfer surface receptors.[6,7] Exosomes can therefore modulate cellular responses and since they change their composition depending on the physiological state of the producing cell, they can exert distinct functional effects on target cells and be potent mediators of cell communication. Exosome-mediated protein complementation has been described in different biological systems. For example, cancer antigens within exosomes are taken up by T cells to elicit antitumor responses once inside their recipients.[8] In this context, we have recently demonstrated that exosomes derived from CMs cultured in glucose

* Corresponding author. Email: pilar.sepulveda.sanchis@gmail.com (P.S.); Email: antonio.diez@igenomix.com (A.D.-J.).

deprivation conditions are able to stimulate angiogenesis of ECs.[9] Additionally, exosomes are able to regulate metabolic activity. For example, hypoxic adipocyte-released exosomes are enriched in enzymes related to lipogenesis such as acetyl-CoA carboxylase, glucose-6-phosphate dehydrogenase, and fatty acid synthase.[10]

Two mechanisms have been identified for exosome release; a constitutive mechanism that is mediated by specific proteins involved in membrane trafficking such as RAB heterotrimeric G-proteins and protein kinase D,[11] and an inducible mechanism that can be activated by several stimuli including increased intracellular Ca^{2+} [12] and DNA damage.[13] Interestingly, conditions of metabolic stress, such as hypoxia, have been found to increase exosome secretion.[14,15] Moreover, it has been recently proposed that microvesicles/exosomes released from CMs are involved in metabolic events in target cells by facilitating an array of metabolism-related processes, including modulation of gene expression.[5]

In this study, we have investigated the possibility that exosomes mediate cellular communication between CMs and ECs during nutritional stress. We found that, under conditions of glucose deprivation, CMs can release exosomes loaded with glucose transporters that, after interaction with ECs, induce glucose uptake and activate glycolytic pathways in recipient cells. This novel communication mechanism underscores the close relationship between CM glucose demand and endothelial glucose transport, allowing a rapid response from ECs to increase glucose transport without the requirement of *de novo* gene transcription and protein synthesis.

2. Methods

Additional information is included in Supplementary material online.

2.1 Animals

Wistar rats (Charles River Laboratories, Inc., Wilmington, MA, USA) were used as breeders, and pups were used for the isolation of neonatal rat CM and ECs. Neonatal transgenic RFP mice (Tg(ACTB-DsRed*MTS)1Nagy/J; The Jackson Laboratory, Bar Harbor, MI, USA) were used also for the isolation of ECs. Neonatal pups of both species were euthanized by decapitation.

2.2 Cell culture

One- to 2-day-old rat pups were sacrificed, hearts were excised, auricles were removed, and ventricles were minced. CMs were isolated using the Worthington Neonatal Cardiomyocyte Isolation System (Worthington Biochemical Corporation, Freehold, NJ, USA). CMs were cultured in Complete DMEM-high glucose, with L-glutamine, sodium pyruvate, 10% FBS, and 1% penicillin–streptomycin. Isolation and culture of ECs from 1- to 2-day-old rat and mouse pups was performed as described. Briefly, the aorta was removed and sectioned into small pieces (1–2 mm) under sterile conditions. Fragments were placed on coverslips or culture plates previously coated with Matrigel (BD Biosciences, San Jose, CA, USA) and cultured with EGM-2 BulletKit (Lonza, Basel, Switzerland). After 1–2 days culture, ECs could be observed sprouting from the explants. H9c2 (2-1) (ATCC) cardiac muscle cells were cultured in DMEM as above. HUVECs (ATCC) and primary adult cardiac rat microvascular ECs (CMVEC; from CellBiologics) were grown in EGM-2 BulletKit.

For experimental conditions, two types of serum-free culture medium were prepared: (i) medium without starvation conditions (−St), containing (DMEM)-high glucose, with L-glutamine, sodium pyruvate, 1% MEM non-essential amino acids, 1% Eagle's MEM vitamin mix (LONZA), 1% insulin-transferrin-selenium (ITS-G, Gibco–Invitrogen, Carlsbad, CA, USA), and 1% penicillin–streptomycin; (ii) medium resulting in starvation conditions (+St), containing DMEM-no glucose, with l-glutamine 1% sodium MEM non-essential amino acids (Sigma-Aldrich), 1% MEM Eagle Vitamin mix (Lonza), ITS-G, and 1% penicillin–streptomycin. All cells were cultured in a humidified incubator at 37°C and 5% CO_2.

2.3 Exosome quantification

2.3.1 Western blot analysis

Tetraspanins are a family of membrane proteins that are very abundant in exosomes. Immunoblotting of tetraspanins CD63, CD9, and CD81 was used to quantify the amount of exosomes released to the culture medium. Exosomal fractions were obtained from equal volumes of culture medium under the different experimental conditions (+/−St) and all of these exosome fractions was utilized for immunoblotting.

2.3.2 Acetylcholinesterase activity

Exosome release was also assessed by the measurement of acetylcholinesterase activity as described previously.[16,17] Briefly, exosomal fractions were obtained from equal volumes of culture medium under the different experimental conditions (+/−St) and 30 μL of the exosome fraction was suspended in 110 μL of PBS. Then, 37.5 μL of this PBS-diluted exosome fraction was added to individual wells of a 96-well flat-bottomed microplate. Next, 1.25 mM acetylthiocholine and 0.1 mM 5,5′-di-thio-bis(2-nitrobenzoic acid, DTNB) were then added to exosome fractions in a final volume of 300 μL, and the change in absorbance at 412 nm was monitored every 5 min. Data are represented as acetylcholinesterase activity after 30 min of incubation at 37°C.

2.3.3 Incell Analyzer quantification

Exosome production in neonatal rat CMs was measured by dual immunolabeling. Cells were cultured in 96-well plates in triplicate in +/−St medium and then fixed with 2% PFA. Cells were labelled with anti-CD63 and anti-desmin (both from Santa Cruz Biotechnology, Inc., Santa Cruz, CA, USA). Secondary antibodies were Alexa Fluor-488 and -555, respectively. Images were acquired with an InCell Analyzer 1000 epifluorescence microscope (GE Healthcare, Cardiff CF14 7YT, UK). A 20× objective was used to collect the fluorescence signals, and a combination of three excitation (EX) and emission (EM) filters were applied to detect DAPI (EX 405 nm/EM 450 nm), green fluorescence from anti-CD63 labelling (EX 475 nm/EM 535 nm), and red fluorescence from anti-desmin detection (EX 530 nm/EM 620 nm). Twenty fields were acquired for each well. Analysis was performed with the InCell Analyzer 1000 Workstation software. Cells were first defined using the nuclear segmentation based on DAPI and the red signal from desmin. The red signal was used to define the cell morphology around the nucleus and to discard desmin-negative cells. Green fluorescence (CD63) was quantified only from desmin-positive cells.

2.4 CD63 and Glut colocalization

Rat neonatal CMs were grown in 96-well plates. After culture in +/−St medium, cells were fixed with 2% PFA and double immunostained with anti-CD63 (secondary antibody Alexa Fluor-488) and anti-Glut1 or anti-Glut4 (secondary antibody Alexa Fluor-647). Cells were imaged live in an InCell Analyzer 1000 high-content analysis system (GE Healthcare) configured with a CCD camera and a 20×/0.45 NA objective. The Q505LP polychroic mirror set was used in conjunction with the following excitation and emission filter combinations: EX 405/20 nm, EM 535/50 nm for DAPI, EX 475/20 nm, EM 535/50 nm for green granules, and EX 475/20 nm, EM 620/60 nm for red granules. Twenty fields were acquired for each well. Analysis was performed as before. For the analysis protocol, we defined a segmentation based on nuclei staining with DAPI, and then we defined the parameters to detect green granules and red granules. The software performed an algorithm calculation to detect the colocalization between the green and red granules (defined as yellow granules), and finaly calculated the number of yellow granules/nuclei.

2.5 *In vitro* exosome functional assays

2.5.1 Transwell approach to measure exosome uptake by CMVECt

We used 24-well plates transwell with 6.5 mm inserts with 0.4 μm polyester membrane permeable supports (Corning, Inc. Costar, NY, USA). In the upper side, we seeded primary CM-CD63-GFP and in the lower chamber, we seeded cardiac microvascular endothelial cells (CMVEC). +/−St media, with or without 14 μM GW4869 (SIGMA), were added to the upper part during 24 h. After that a total of 3×10^5 CMVEC/well were seeded at the bottom part of 24-well plates and EGM-2 BulletKit was added. Shortly after, the CM-CD63-GFP inserts with +/− 24 h of St media were placed on the top of CMVEC cultures. After 24 h incubation (a total of 48 h with/without starvation for CM-CD63-GFP), inserts were removed and the intensity of GFP fluorescence was determinated in the CMVEC with InCell Analyzer. Images were acquired with an InCell Analyzer 1000 epifluorescence microscope (GE Healthcare). A 20× objective was used to collect the fluorescence signals in living CMVEC and a combination of two EX and EM filters were applied to detect Hoescht (EX 405 nm/EM 450 nm) and green fluorescence from CD63-GFP labelling (EX 475 nm/EM 535 nm). Twenty fields were acquired for each well. Analysis was performed with the InCell Analyzer 1000 Workstation software. Cells were first defined using the nuclear segmentation based on Hoescht and green intensity/cell was determinated.

2.5.2 Glucose uptake

Rat primary CMVECs were cultured in MatriPlate 96-well microplates (GE Healthcare). Measurement of 2-(*N*-(7-nitrobenz-2-oxa-1,3-diazol-4-yl) amino)-2-deoxyglucose (2-NBDG, Invitrogen) uptake was performed as described[18] with minor modifications. Briefly, cells were washed with PBS and +St medium was added for 2 h. Then, 20 μg/mL of exosomes (or PBS control) were added to each well followed by incubation for 30 min at 37°C. Cells were washed and DMEM-no glucose containing l-glutamine and 150 μg/mL of 2-NBDG was added, followed by incubation for 30 min at 37°C. Cells were then washed and fixed in 2% paraformaldehyde (PFA) for imaging. The acquisition of samples was performed by epifluorescence microscopy as before. A 20× objective was used to collect the fluorescence signals, and a combination of two EX and EM filters was applied to detect DAPI (EX 405 nm/EM 450 nm) and green fluorescence from 2-NBDG (EX 475 nm/EM 535 nm). Forty fields were acquired for each well. Image analysis was performed as before using a platform to detect intracellular 2-NBDG granules. To define the cells, a nuclear segmentation from DAPI was used and quantification of 2-NBDG granule was performed. To quantify the 2-NBDG uptake level for each field, 2-NBDG granule count/cell was measured.

Glucose transport can be inhibited with the Glut inhibitor fasentin.[19] To inhibit exosomal Glut, an aliquot of the exosome fraction was incubated for 1 h with 100 μM fasentin. Then, a 20 μg/mL sample (10 μL stock exosome solution) of Glut-inhibited exosomes was added to CMVEC in the final volume of 310 μL (3.22 μM fasentin, final concentration) and incubated for 30 min at 37°C. Cells were washed and the 2-NBDG capture assay was performed.

2.5.3 Lactate dehydrogenase assay

Lactate dehydrogenase (LDH) activity was measured using the Lactate Dehydrogenase Activity Assay Kit (Sigma). For determination of exosome LDH activity, the total exosome fraction obtained from 100 mL of primary CM culture medium with or without (+/−St) glucose starvation was suspended in LDH Assay Buffer. For CMVEC LDH activity, cells were grown to confluence in six-well plates. The total exosome fraction obtained from 100 mL of primary CM culture medium, or 100 μL of PBS (control), was added directly to CMVEC cultures. After 30 min of incubation at 37°C, cells were quickly washed with cold PBS and 150 μL of LDH Assay Buffer was added directly to each well. Results show the average of two independent experiments.

2.5.4 Pyruvate quantification

Pyruvate quantification of CMVEC and culture media was carried out with the Pyruvate Assay Kit (Abcam). CMVECs were grown to confluence in six-well plates. Then, cells were washed in PBS and overlaid with assay media containing DMEM-no glucose, no pyruvate (Invitrogen), all supplements from EGM-2 BulletKit, and d-(+)-glucose (1 g/L). Immediately after, total exosome fraction obtained from 100 mL of primay CM culture media, or 100 μL of PBS (control), was added directly to the assay medium. After 30 min incubation at 37°C, a sample was taken from the culture medium for quantification. Cells were washed with cold PBS and 100 μL of Assay Buffer was added directly to each well. Results show the average of three independent experiments.

2.6 H9c2-(GLUT4, GLUT1)-GFP and HUVEC co-culture: quantification of GFP intercellular trafficking

To quantify the amount of Glut4 and Glut1 moving from H9c2 cells to HUVEC under the different experimental conditions (+St or −St), we performed co-culture assays with H9C2-GLUT4-GFP or H9C2-GLUT1-GFP and HUVEC. HUVECs were grown in 24-well plates in duplicate. Once HUVEC reached 50% confluence, H9C2-GFP cells were added. Twenty-four hours later, culture medium was replaced with +St or −St medium. After a further 24 or 48 h of culture, cells were fixed in 2% PFA and stained with anti-GFP (secondary antibody Alexa Fluor-488, green) and anti-CD31 (secondary antibody Alexa Fluor-555, red). Images were captured as before with an InCell Analyzer 1000 high-content analysis system using a 40× objective, and a combination of three EX and EM filters was applied to detect DAPI (EX 405 nm/EM 450 nm), green fluorescence from anti-GFP (EX 475 nm/EM 535 nm), and red fluorescence for anti-CD31 detection (EX 530 nm/EM 620 nm). Twenty fields were acquired for each well. Image analysis was performed as before; to define the cells, a nuclear segmentation based on the DAPI signal and the red signal from HUVEC CD31 was performed. The red signal was used to define the cell morphology around the nucleus, and to discard CD31-negative cells. Green fluorescence was quantified only from CD31-positive cells.

2.7 Statistics

Data are expressed as mean ± SD. Comparisons between experimental conditions were performed with Student's paired *t*-test, and ANOVA for multiple comparisons. Analyses were conducted with SPSS and GraphPad Prism 5 software. Differences were considered statistically significant at $P < 0.05$ with a 95% CI.

3. Results

3.1 Glucose starvation increases synthesis and secretion of exosomes in cultured CMs

CMs can produce microvesicles/exosomes containing nucleic acids capable of altering the activity of target cells.[5] To study this phenomenon during metabolic crisis, we analysed the synthesis and secretion of exosomes from cultured CMs subjected to glucose starvation. Exosomes obtained from neonatal murine CMs cultured for 48 h in control (−St) or glucose starvation media (+St) were examined by EM to determine their shape, average size, and relative abundance. We found increased relative abundance of exosomes under starvation conditions (*Figure 1A*). Western blot (WB) analysis of exosome fractions using antibodies against tetraspanins CD63, CD9, and CD81 confirmed the presence of exosome-specific antigens under both conditions, although glucose starvation stimulated the secretion of exosomes (*Figure 1B*). The image analysis showed a significant increase in tetraspaning signals when exosomes came from +St CMs. Moreover, the production of

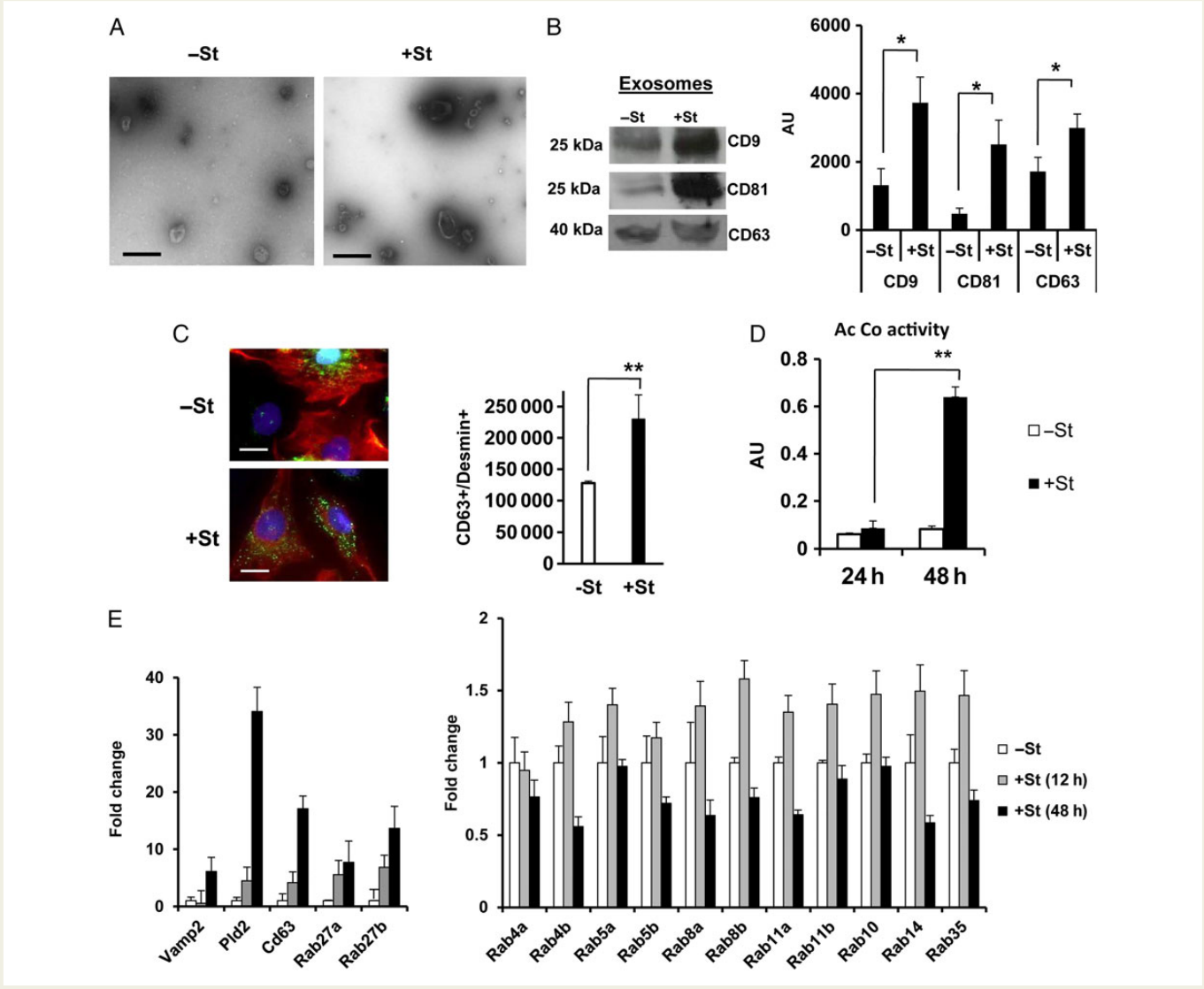

Figure 1 Glucose starvation increases synthesis and secretion of exosomes in rat neonatal CMs. (*A*) EM of isolated exosomes collected from culture media of glucose-starved (+St) or glucose-replete (−St) cardiomocytes after 48 h. Scale bars, 100 nm. (*B*) Western blot of tetraspanin expression in exosomes obtained from 30 mL of culture medium from neonatal cardiomyoyctes cultured as in (*A*). Graphic shows optical density quantification of WB signals ($n = 3$). (*C*) Fluorescence microscopy of fixed cardiomyocytes stained with anti-CD63 (green), anti-desmin (red), and DAPI (nucleus, blue). Scale bar: 10 μm. Graph denotes InCell fluorescence quantification of green spots (CD63+) in desmin+ cells. Cells were cultured for 24 h as in (*A*) ($n = 3$). (*D*) Quantification of acetylcholinesterase activity of exosomes obtained from equal amounts (30 mL) of CM culture medium with (+St) or without (−St) glucose starvation ($n = 6$). (*E*) qPCR analysis of genes implicated in secretory pathways from CMs cultured for 12 h (grey bars) or 48 h (black bars) of glucose starvation (+St). Results are expressed relative to −St culture (white bars, $n = 3$). *$P < 0.05$ in *B*, ** $P < 0.01$ in *C* and *D*. *t*-Test was used in all comparisons.

exosomes was greater in CMs cultured in glucose-deprived medium (+St) compared with glucose-replete medium (−St), as determined by InCell quantification of CD63 staining (green) in desmin-positive (red) cells (*Figure 1C*). Acetylcholinesterase activity is specific to exosomes.[17] To validate the increased exosome secretion in glucose-starved CMs, we measured acetylcholinesterase activity in exosome fractions obtained from neonatal CMs in −St and +St conditions. Results showed that 48 h of glucose starvation significantly increased exosome acetylcholinesterase activity with respect to control cultures, indicating greater exosome secretion (*Figure 1D*). Previous studies have linked the activity of several genes to functional cellular secretory pathways.[20] We used qPCR analysis to measure the expression of several of these genes in glucose-starved CMs. As anticipated, secretory-related genes were up-regulated in +St-cultured neonatal CMs (*Figure 1E*). Phospholipase D hydrolyzes phosphatidylcholine to generate choline and phosphatidic acid, which is implicated in many cellular functions including exocytosis and endocytosis, and directly activates a number of proteins such as mTOR.[21] Phospholipase D2 (PLD2) is present in exosomes and PLD2 activity correlates with the amount of exosomes released by cells.[22] Accordingly, PLD2 mRNA was up-regulated in glucose-starved CMs.

Rab GTPases are a large family of small GTPases that control intracellular vesicular traffic.[23] Specifically, Rab27a and Rab27b control different steps of the exosome secretion pathway.[24] We found increased Rab27a and Rab27b mRNA levels in glucose-starved CMs (*Figure 1E*).

Vesicle-associated membrane protein-2 (VAMP-2), a Golgi SNAP receptor (SNARE) complex protein involved in intracellular Glut4 trafficking,[25] was also up-regulated in starved CMs (*Figure 1E*). Other RabGTPases were increased at 12 h in glucose-starved CMs, although they returned to normal levels or were slightly reduced at 48 h (*Figure 1E*). Furthermore, we had analysed during routine exosome purification the content of histone H4 in exosomal fractions derived from rat neonatal primary CM cultures and H9C2 (see Supplementary material online, *Figure S1A* and *B*). This allowed us to discount apoptotic bodies' contamination. Also, during the experimental set-up, we performed analysis of cell death during starvation by flow cytometry analysis for Annexin V/propidium iodide (PI) for cultures after 48 h incubation with +/−St media. We did not find significant levels of cell death in either primary CM or H9C2 cultures (see Supplementary material online, *Figure S1C* and *D*).

3.2 Exosome transfer from CMs to CMVEC

As previously described for exosome-tracking studies,[26] we transduced primary rat CM with a CD63-GFP lentivirus to generate CM-CD63-GFP cells producing exosomes with GFP fused to CD63 (*Figure 2A*). The percentage of transduced cells was determined by flow cytometry (79.7%) and corroborated by confocal microscopy (*Figure 2B*). We hypothesized that glucose starvation-induced CM stress would provoke an exosome-mediated response directed to CMVEC responsible for metabolic fuel transport from blood. To determine the capacity for CMs to transfer exosomes to CMVEC, we

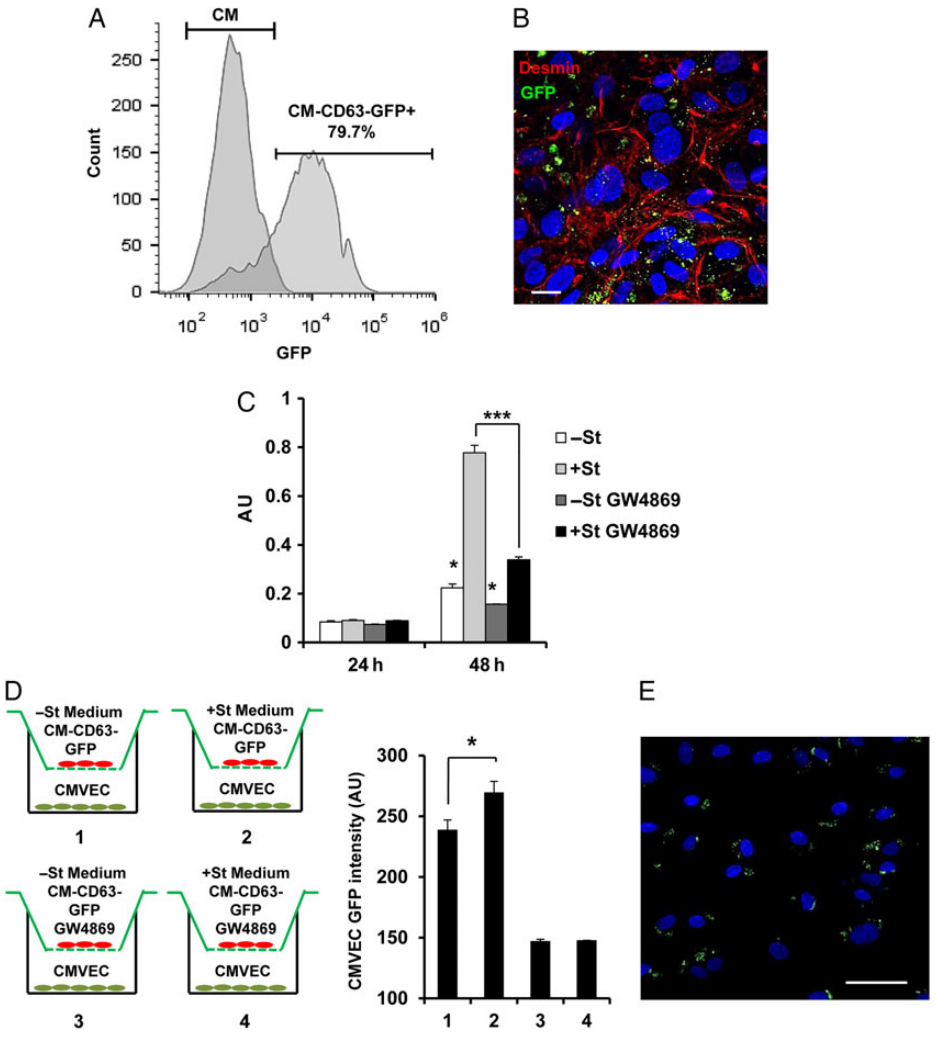

Figure 2 Exosome traffic from primary CM to CMVEC is increased in +St conditions. (*A*) Primary CMs were transfected with pCT-CD63-GFP. FACS analysis of transfected cells showing % GFP-positive cells. This cell population was termed CM-CD63-GFP. (*B*) CM-CD63-GFP immunostaining with anti-desmin (red), anti-GFP (green), and DAPI (blue). Scale bar: 10 μm. (*C*) Quantification of acetylcholinesterase (Ac Co) activity of exosomes obtained with Exoquick-TC from equal amounts (20 mL) of conditioned medium from primary CM cultured 24/48 h in +/−St media in the presence or absence of 14 μM GW4869 ($n = 3$). AU, arbitrary units. (*D*) CM-derived exosome uptake by CMVEC in a transwell approach with 0.4 μm membrane permeable inserts with CM-CD63-GFP. CMVECs in EGM-2 BulletKit were co-cultured during 24 h with CM-CD63-GFP (with previous 24 h of +/−St media, 1 and 2; and with 14 μM GW4869, 3 and 4). After that, CMVEC GFP intensity was measured with the InCell Analyzer. The graph shows the result of GFP intensity quantification ($n = 3$). (*E*) Representative image of lane 2 from (*D*). Living CMVEC with nucleus in blue (Hoescht) and CD63-GFP exosomes from CM-CD63-GFP with green fluorescence. Scale bar: 50 μm. *$P < 0.05$; ***$P < 0.001$. *t*-Test.

designed a transwell approach experiment. GW4869 has been described as an inhibitor of N-SMase (neutral sphingomyelinase),[27] with a potent role in the exosome secretion process.[28,29] First, we tested the potential of 14 μM GW4869 (Sigma) to inhibit exosome secretion in primary CM with or without glucose starvation (+/−St; *Figure 2C*). We observed that after 48 h of starvation, exosome secretion was drastically decreased when cells were treated with 14 μM GW4869. Given that glucose deprivation increased the secretion of exosomes in primary CM, we quantified exosome CD63-GFP transfer from CM-CD63-GFP to CMVEC (*Figure 2D* and *E*). CM-CD63-GFP were cultured in transwell inserts during 24 h with +/−St medium and +/− 14 μM GW4869. After that, inserts were co-cultured 24 h with CMVEC previously seeded at the bottom part of transwell, to allow interaction of CMVEC with exosomes derived from CM-CD63-GPF generated at different culture conditions. After co-culture, we detected GFP fluorescence in CMVEC and we observed a significant increase in GFP signal in these cells when CM-CD63-GFP at the upperside of transwell was cultured with +St media. Moreover, when CM-CD63-GFP were treated with GW4869, the CMVEC GFP intensity was drastically reduced, which indicates that GFP fluorescence came from CD63-GFP structures.

To find *in vivo* evidence of this exosomes trafficking, we investigated by EM the presence of exosomes in the perivascular space between CM and EC in rat heart tissue (see Supplementary material online, *Figure S2A–C*). As described similarly by Sahoo *et al.*,[30] we identified exosomes-like vesicles in a close location to the perivascular space between the CM and EC.

3.3 Exosomes from starved CMs increase glucose uptake of CMVEC

Since exosome trafficking from primary CM to CMVEC could be modulated by glucose, we next examined whether exosomes could affect glucose transport of CMVEC. Thus, exosomes collected from primary CM culture medium (with or without prior glucose starvation) were added to CMVEC and glucose uptake of the fluorescent deoxyglucose analogue, 2-NBDG, was measured after incubation for 30 min. Interestingly, whereas CMVEC treated with exosomes collected from CMs in glucose-replete medium exhibited glucose uptake similar to control (no exosomes) conditions, exosomes from glucose-depleted (+St exos) CM cultures provoked a significant increase in endothelial glucose uptake (*Figure 3A*), suggesting that exosomes from starved CMs were loaded with molecules able to modify CMVEC metabolism.

Glut1 and Glut4 are present in intracellular CM vesicles. We assessed the presence of Glut proteins in CM-derived exosomes by western blotting and EM. For identifying exosomal GLUTs by WB, exosomes were obtained by ultracentrifugation from the culture medium of neonatal rat CM with or without 48 h of glucose starvation (+/−St) and 10 μg of exosome protein extract was used for immunoblotting in each lane. Greater expression of Glut1 and Glut4 glucose transporters were observed in exosomes collected from glucose-depleted CM cultures compared with those obtained from non-starved cells (*Figure 3B*). The image analysis software to quantify the optical density of the bands on the blot showed a significant increase in GLUT4/CD63 and GLUT1/CD63 signals when exosomes came from +St CMs. Immunogold labelling and EM confirmed the presence of Glut proteins in exosomes isolated from starved CM medium (*Figure 3C* and see Supplementary material online, *Figure S3A* for uncropped images). In accord with results from western blotting, no positive labelling was detected in exosomes from non-starved CM medium (data not shown) .

To determine whether the increase in CMVEC glucose uptake was elicited by exosomal Gluts, CM-derived exosomes were treated with the Glut inhibitor fasentin[19] before measuring levels of 2-NBDG uptake. Similar to previous results (*Figure 3A*), CMVEC treated with exosomes isolated from glucose-starved CM (+St Exos) exhibited an increase in 2-NBDG uptake over control (no exosomes) and glucose-replete-derived exosomes (−St Exos, *Figure 3D*). Conversely, incubation of an equivalent exosome fraction with fasentin (100 μM fasentin, 1 h; +St Exos + fas) ablated 2-NBDG uptake, suggesting that the activity of exosomal Gluts is responsible for the increase in 2-NBDG uptake. To discount the possibility that inhibition of uptake was due to the residual fasentin added to the CMVEC with the exosomes, we treated those cells with the same final concentration of fasentin (3.22 μM) in the absence of exosomes. Results demonstrated an equal uptake of 2-NBDG in the presence of fasentin with respect to the control (*Figure 3D*).

3.4 Transfer of Gluts from CMs to ECs

Dual immunocytochemical labelling of neonatal rat CMs cultured in −St or +St demonstrated the presence of intracellular structures that stained positive both for CD63 and Glut1 or Glut4, respectively (yellow dots; *Figure 4A*). InCell quantification of yellow colocalization signals revealed that glucose deprivation increased the number of intracellular CD63-positive structures containing Glut1 or Glut4 in primary CMs, suggesting that glucose starvation induces the loading of exosomes with these transporters (*Figure 4A*).

To further investigate the relationship between increased glucose uptake and exosome-mediated transfer of glucose transporters, we generated H9c2 reporter cell lines expressing GLUT1 or GLUT4 fused to GFP, allowing us to evaluate Glut trafficking to ECs by time-lapse confocal microscopy. Analysis of co-cultures of H9C2-GLUT1-eGFP or H9C2-GLUT4-eGFP cells with DsRed-labelled mouse ECs demonstrated that, mainly under starvation conditions, ECs were able to capture H9c2-derived GLUT1-GFP and GLUT4-GFP transporters (*Figure 4B*). Furthermore, once internalized in ECs, GLUT-GFP proteins were clustered, transported along the cytoplasm, and then disaggregated (see Supplementary material online, *Movies S1* and *S2*). We next quantified GLUT1- and GLUT4-GFP transfer in co-cultures of H9C2-GLUT1-GFP or H9C2-GLUT4-GFP and HUVEC. InCell quantification of the GLUT1- and GLUT4-GFP signal in co-cultured HUVEC confirmed the internalization of Glut transporters from H9c2 cells (green) in ECs (CD31-positive, red). As before (*Figure 2D*), we observed differences in the extent of exosome transfer between cells grown in complete or glucose-deprived media; accordingly, transfer of GLUT-GFP was significant in a glucose-dependent manner at 48 h. GLUT4-GFP expression was 7.43 ± 7.40 in −St and 248 ± 41.04 in +St ($P < 0.001$, $n = 4$; *Figure 4C*) in HUVEC, and GLUT1-GFP expression in HUVEC was 23.90 ± 7.57 in −St and 260 ± 19.67 in +St ($P < 0.001$, $n = 4$; *Figure 4D*). It is noteworthy that H9c2 is an immortalized myoblastic cell line and we cannot discard differences with primary CM, although this mechanism can potentially not be exclusive of CM and can be active in other cells and tissues.

3.5 Exosomes from CM induce glycolytic activity in CMVEC

Thus far, our results show that exosomes from glucose-starved CM increase glucose uptake in CMVEC. This increase of glucose in the endothelium does not reflect the metabolic needs of the endothelium itself;

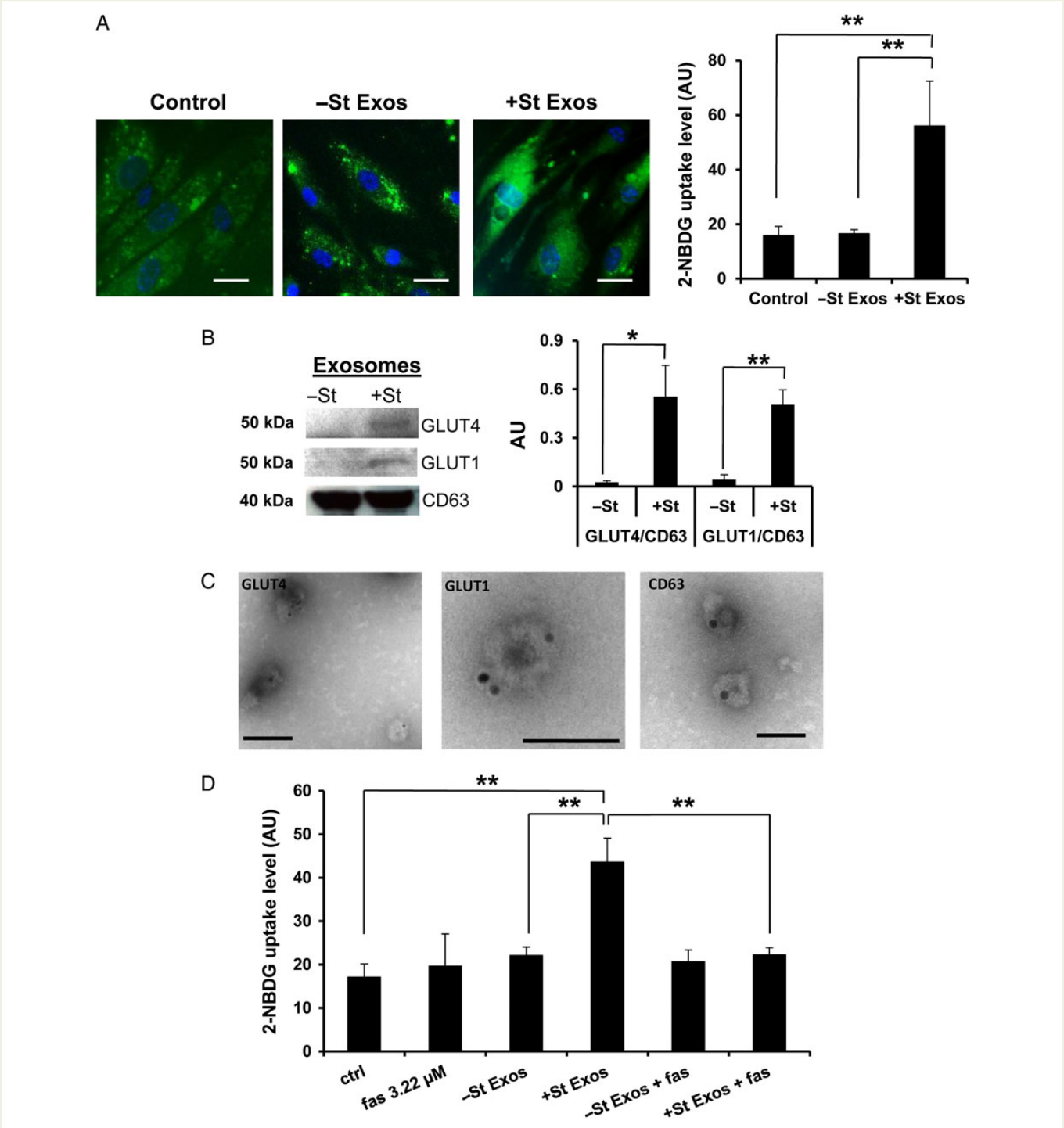

Figure 3 Exosomes from starved rat neonatal CMs increase 2-NBDG uptake in CMVEC. (*A*) Capture of 2-NBDG (green) by CMVECs after 30 min of treatment with 20 μg/mL exosomes isolated from neonatal rat CM culture media with (+St Exos) or without (−St Exos) 48 h starvation. Scale bar: 20 μm. Graph shows InCell quantification of 2-NBDG capture ($n = 6$). (*B*) Western blotting of Glut1 and Glut4 in exosomes isolated from CM culture media after 48 h with (+St) or without (−St) starvation. Graphic shows optical density quantification of WB signals ($n = 3$). (*C*) Immunogold EM of CD63, Glut4, and Glut1 in exosomes isolated from CM culture media after 48 h of glucose starvation. Scale bars, 70 nm. Uncropped images are showed in Supplementary material online, *Figure S3A*. (*D*) Incell quantification of 2-NBDG uptake by CMVEC. Where indicated, cells were pretreated for 30 min before 2-NBDG uptake assay. Ctrl: PBS; fas: fasentin; −/+St Exos: 20 μg/mL of exosomes isolated from 48 h-cultured −/+St CMs; −/+St Exos + fas: 20 μg/mL of exosomes isolated from 48 h-cultured −/+St CMs. Where indicated, exosome fractions were incubated for 1 h with 100 μM fasentin before adding to CMVEC. *$P < 0.05$, **$P < 0.01$ in *B*. *t*-test was applied in *B*. One-way ANOVA was applied in *A* and *D*, and posterior *t*-test for pair comparisons.

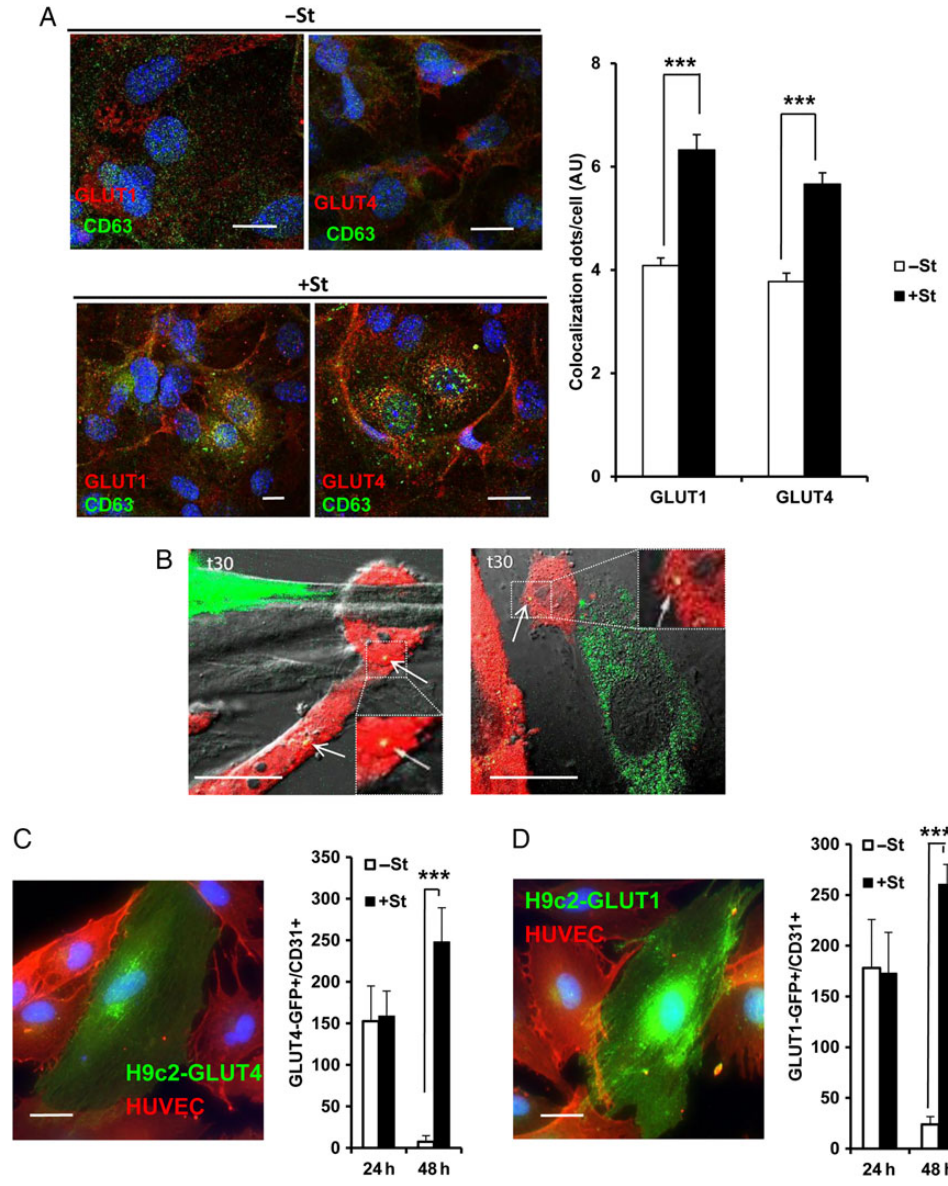

Figure 4 Glut transfer from CMs to ECs. (*A*) Rat neonatal CMs were cultured in +St or −St for 24 h. Double immunostaining with anti-Glut4 or anti-Glut1 (red) and CD63 (green) antibodies. Scale bar: 10 μm. Graph shows InCell quantification of yellow co-localization signals ($n = 2$). A total average of 6798 ± 140 cells were analysed per each treatment. (*B*) Time-lapse confocal microscopy of murine endothelial (ACTB-DsRed) cells (red) co-cultured with H9C2-GLUT4-GFP cells (green, left panel) or H9C2-GLUT1-GFP cells (green, right panel), previously starved for 2 h. White arrows show transfer of Glut from H9C2 CMs into ECs (see Supplementary material online, *Movies S3* and *S4*). Time (*t*) in minutes. Scale bar: 20 μm. (*C*) Co-culture of H9C2-GLUT4-GFP and HUVEC with (+St) or without (−St) glucose starvation. Immunostaining with anti-GFP (green) and anti-CD31 (red) antibodies. Scale bar: 20 μm. Graph shows the InCell quantification of GFP fluorescence from GLUT4-GFP in CD31+ cells (red, $n = 4$). (*D*) Co-culture of H9C2-GLUT1-GFP and HUVEC with (+St) or without (−St) glucose starvation. Immunostaining with anti-GFP (green) and anti-CD31 (red) antibodies. Scale bar: 20 μm. Graph shows the InCell quantification of GFP fluorescence from GLUT1-GFP in CD31+ cells (red, $n = 4$). ***$P < 0.001$. *t*-test.

rather, it is a response to the metabolic demands of CMs. ECs rely on aerobic glycolysis to sustain growth, which is characterized by glucose consumption and lactate production.[31] Interestingly, we found that CM exosomes significantly increased CMVEC LDH activity over control treatment (*Figure 5A*) and this was exacerbated by exosomes from +-St-conditioned medium (*Figure 5A*). As previous studies have reported that exosomes contain proteins related to cell metabolism, we next investigated the presence of LDH and glyceraldehyde-3-phosphate dehydrogenase (GAPDH) proteins in primary CM-derived exosomes. Western blot analysis demonstrated a marked increase of both proteins in exosomes derived from glucose-starved cultures (*Figure 5B*). Furthermore, exosomal fractions obtained from primary CM exhibited functional LDH activity (*Figure 5C*). Although no significant differences were found in the activity of LDH in equivalent quantities of exosomes (30 μg +/−St Exos), we observed increased LDH activity in the total exosome fraction (*Figure 5C*), indicating that this increase is directly related to increased secretion of exosomes. LDH catalyses the reversible interconversion of lactate and pyruvate, two metabolites that are

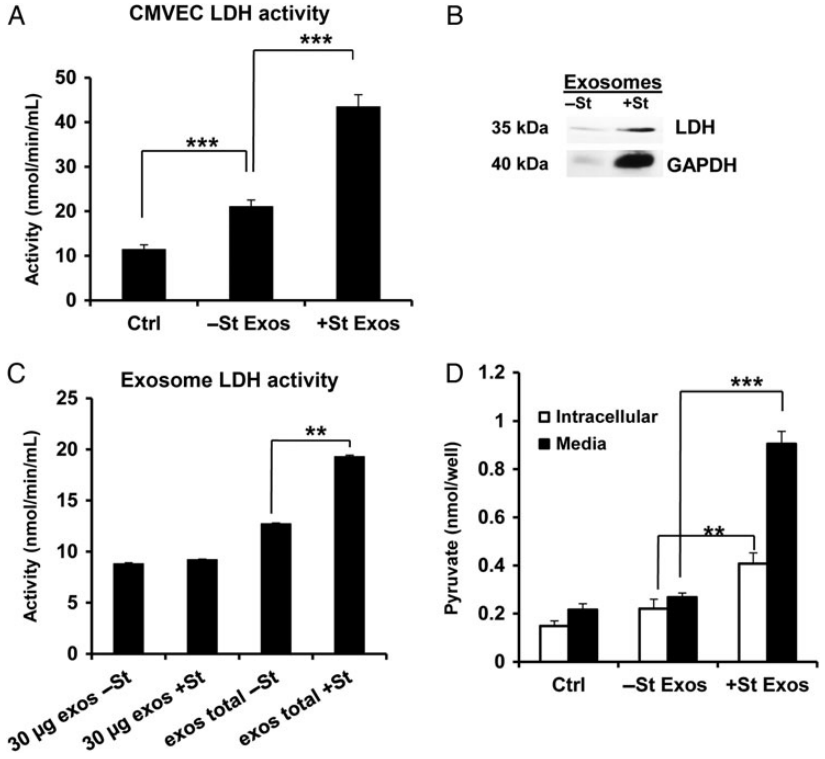

Figure 5 Exosomes from primary CM increase glycolytic activity of CMVEC. (*A*) LDH activity assay in CMVEC after 30 min incubation with total exosome fraction obtained from primary CM with or without 48 h starvation (Exos +St or −St). PBS (100 µL) was added to CMVEC as a control ($n = 4$). (*B*) Western blotting for total exosome fraction obtained from primary CM with or without 48 h starvation (+St or −St). (*C*) LDH activity assay for exosome fraction obtained from primary CM with or without 48 h starvation (+St or −St). Total fraction was obtaind from 100 mL of primary CM culture medium (total −/+St Exos, $n = 4$). (*D*) Pyruvate quantification in CMVEC culture after 30 min incubation with total exosome fraction obtained from primary CM with or without 48 h starvation (Exos +St or −St). PBS (100 µL) was added to CMVEC as a control. White bars represent intracellular pyruvate and black bars represent the pyruvate diffused into the culture medium ($n = 4$). $^{**}P < 0.01$, $^{***}P < 0.001$. One-way ANOVA was applied and posterior *t*-test for pair comparisons.

essential for metabolic homeostasis in the heart. We measured CMVEC pyruvate production in the presence of primary CM-derived exosomes. We found that exosomes from glucose-starved CM-conditioned medium (+St Exos) increased both the production (measured as intracellular pyruvate) and the diffusion (measured as pyruvate detected in media) of pyruvate in CMVEC with respect both to control conditions and to exosomes collected from glucose-replete medium (*Figure 5D*; intracellular pyruvate: 0.15 ± 0.01 in control, 0.18 ± 0.008 in −St Exos, 0.29 ± 0.08 in +St Exos; ANOVA, $P < 0.001$, $n = 4$); pyruvate in media: 0.21 ± 0.009 in control, 0.24 ± 0.007 in −St Exos, 0.72 ± 0.03 in +St Exos (ANOVA $P < 0.001$, $n = 4$). ECs have a paucity of mitochondria; in consequence, pyruvate is not utilized with high efficiency by the mitochondrial oxidation pathway. Thus, the fast induction in endothelial pyruvate production likely does not reflect the metabolic needs of ECs but, instead, provides pyruvate to the extracellular medium through plasma membrane diffusion (*Figure 6*).

In our model, metabolic needs are generated in CM but not in ECs. To test these, we performed 2-NBDG uptake in 24 h glucose-starved CMVEC and we did not observed change in 2-NBDG uptake when CM-derived exosomes were added, indicating that EC need conditions of glucose availability to respond to CM metabolic demands (see Supplementary material online, *Figure S3B*). Similar to these, we did not observe changes in CMVEC LDH activity when CM-derived exosomes were added (see Supplementary material online, *Figure S3C*).

4. Discussion

In this work, we examined how CM-derived exosomes can alter glucose transport in ECs. We show that under energetic stress, CMs increase the synthesis and secretion of exosomes, which are internalized by ECs. These exosomes mediate the transfer of functional glucose transporters and glycolytic enzymes. ECs exposed to exosomes secreted by glucose-starved CMs increase glucose uptake and pyruvate synthesis, which could potentially support CM nourishment (*Figure 6*). Previous reports have shown that myocardial tissue in the adult heart secretes exosomes (reviewed in Sluijter *et al.*[32]). Our findings suggest an intimate relationship between nutrient sensing and exosome release. Recent studies have indicated a significant overlap in the molecular machinery used in exocytosis and exosome trafficking. In addition, autophagy and nutrient sensing are closely related processes, and imbricated to vesicle transport. Thus, similar mechanisms may be operating in both situations.[33,34,35] All of these mechanisms involves both small GTPases and the membrane fusion machinery. We identified several molecules involved in multivesicular body (MVB) biology that were strongly up-regulated by starvation. Rab27a and Rab27b have an important role in MVB intracellular trafficking and exosome secretion,[24] by promoting the targeting of MVBs to the cell periphery and their subsequent docking at the plasma membrane. PLD2 modulates exosome trafficking by controlling the budding of intralumenal vesicles

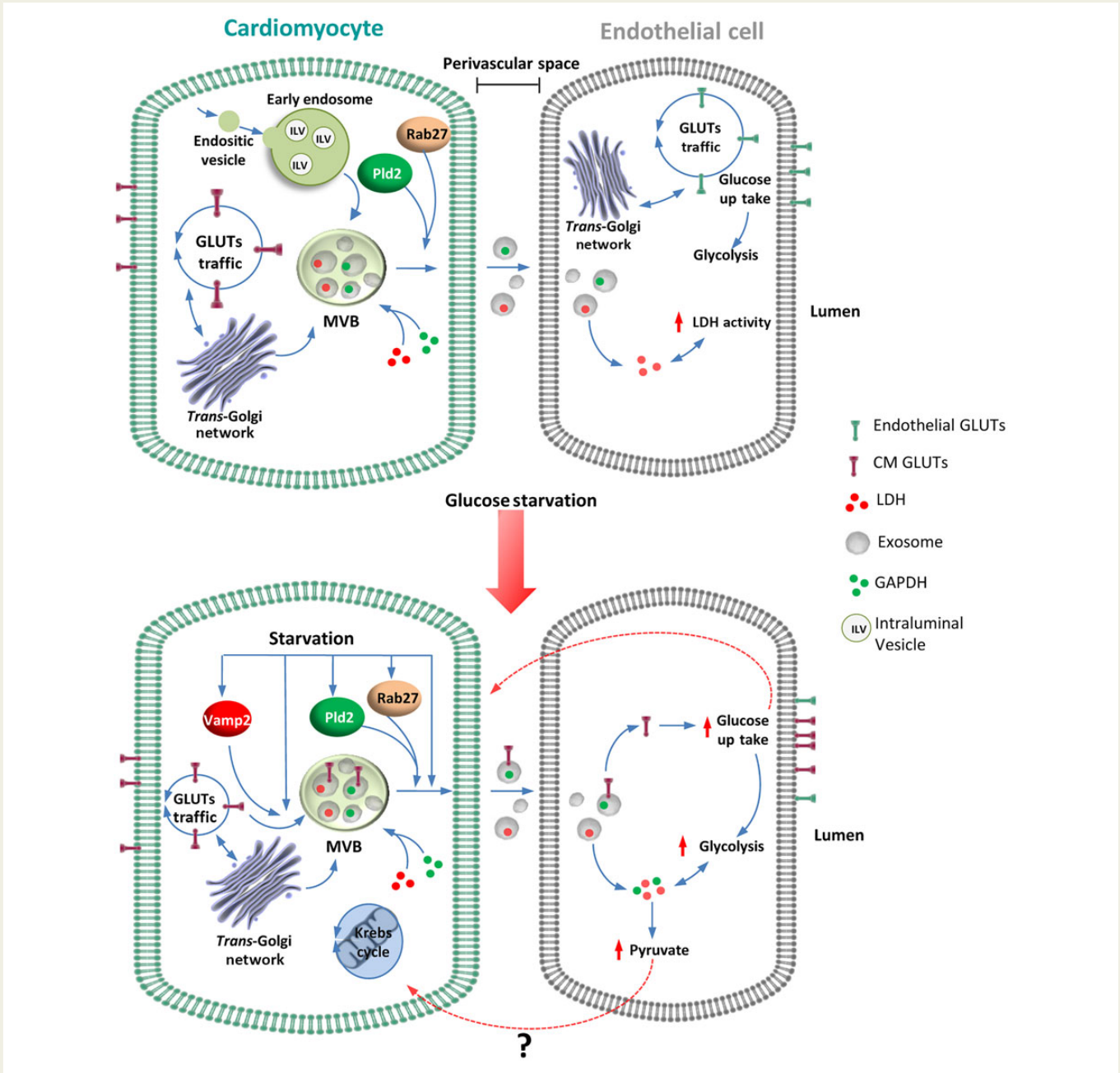

Figure 6 CM–endothelial exosome crosstalk. Schematic diagram showing the intimate contact between CMs and ECs, pivotal for metabolic coupling. In the presence of appropriate levels of glucose in CMs, there is a basal traffic of exosomes from CMs to ECs. Under these conditions, intracellular Glut traffic is independent of the exosome secretion pathway and exosomes do not contain Gluts. Stress signal caused by glucose starvation induces an increase in exosome secretion and a coupling between the exosome secretion pathway and Glut vesicular traffic, potentially mediated by molecules such as PLD2/Rab27 and VAMP-2, respectively. In these situations, exosomes are loaded with Gluts that in turn are able to induce functional changes in the endothelial glycolytic pathway.

into MVBs,[36] and its activity correlates with the release of exosomes.[22] Of interest, we found that the expression of other Rab GTPases, including Rab35 and Rab14, were up-regulated at 12 h of starvation but then down-regulated at 48 h. Some of these proteins (Rab5a and Rab14) play a role in targeting endosomal traffic towards lysosomes.[37–39] Also, Rab5 and Rab11 play a significant role in autophagosome formation[40] and, together with Rab8b, in autophagosome maturation. Additionally, several RabGTPases, such as Rab5, Rab10, and Rab14, regulate glucose transporter traffic.[41] This pathway convergence integrates autophagy, vesicle transport, and exosomal synthesis, and secretion can explain the differential regulation at RabGTPases that we found at different time points. It is conceivable that the absence of glucose generates stress signals leading to a convergence of the Glut trafficking pathway and the exosome secretion pathway, generating Glut-loaded exosomes. Our observation of strong transcriptional up-regulation of VAMP-2, a SNARE protein, in glucose-starved CMs is consistent with its association with Glut4 trafficking,[42,43] and its function in mediating vesicle fusion with the plasma membrane.[44] Collectively, this

up-regulation of genes involved in MVB targeting and fusion to the plasma membrane is in agreement with the increased exosome release observed under glucose starvation and is consistent with Glut trafficking. Protein translocation from CM to EC can potentially be favoured due to the little metabolic capacity of the microvascular cells. Mitochondrial content in ECs is modest compared with other cell types with higher energy requirements.[45] Protein synthesis and folding requires a high amount of energy that, in some situations, can be impaired in EC due to the relatively low energetic capacity of these cells compared with CM. Thus, an asymmetric glycolysis in the endothelial face close to the CM could facilitate pyruvate difussion to CM. Exosome-mediated intercellular transport of functional proteins between cells has been identified in other biological contexts including cancer, where microvesicles containing an active oncogene (oncosomes) serve as vehicles for rapid intercellular transfer of the transforming activity between tumour cells or as a means to reduce cell proliferation by transfer of tumour suppressors.[46] Additionally, functional components of Notch and Wnt signalling pathways are secreted in exosomes to modulate cell behaviour in trans.[47–49] We propose that in an analogous fashion, glucose uptake from the endothelium to CMs could be regulated, at least in part, by short range exosome communication. This mechanism would allow a fast response from the endothelium without the need of novel protein synthesis. Thus, energy demand of CMs would increase glucose metabolism of the associated ECs via exosome-mediated Glut1 and Glut4 intercelular translocation.

In addition, other enzymes of glucose metabolism, including LDH and GAPDH, were also found in exosomes. Consequently, exosomes derived from glucose-starved CMs had increased LDH activity, leading to an increase in pyruvate in endothelium. ECs obtain energy from aerobic glycolysis. Pyruvate can diffuses through the membranes.[50] Thus, potentially increased production of pyruvate in the ECs would result in locally diffusion towards CMs for oxidation by the Krebs cycle as we schematized in *Figure 6*. In our model, the metabolic stress was generated in CM, but not in the ECs. We studied the functional consequence of generating metabolic stress in ECs by incubating 24 h with glucose-deprived media and we saw no significant difference in both the uptake of 2-NBDG and LDH activity when +/− St exosomes from CM (or H9C2) were added (see Supplementary material online, *Figure S3B* and *C*). This means that in our proposed model, ECs must have adequate levels of glucose to respond to signals sent from CMs through exosomes. Interestingly, treatments that are able to reduce blood glucose, such as metformin and glitazones, also work as energy restriction mimetics. These drugs might potentially activate tissue–endothelial metabolic complementation, suggesting another mechanism to control glucose homeostasis. Thus, this study has potential implications in pathologies, such as type 2 diabetes and obesity, and also the insulin resistance that appears in ageing.

Supplementary material

Supplementary material is available at *Cardiovascular Research* online.

Authors' contributions

A.D.-J. and N.A.G. designed all research and performed experiments. A.D.-J., N.A.G., and P.S. analysed data and wrote the paper. J.M.-A. perform EM histology.

Acknowledgements

We thank RETICS Program (RD12/0019/0025) cofounded by FEDER "una manera de hacer Europa", and A. Hernández and M. Soriano at the Core Facility of Confocal Microscopy and Electron Microscopy-Centro de Investigación Príncipe Felipe, respectively. We thank F. Sanchez-Madrid for the gift of CD63-GFP plasmid, D.E. James for the gift of GLUT4-GFP plasmid, and C. Thery for immunostaining protocols.

Conflict of interest: none declared.

Funding

N.G. acknowledges a fellowship from Erasmus Mundus Eurotango Program. A.D.-J. acknowledges support from the *Ramon y Cajal* program (RYC-2008-02378). P.S. acknowledges support from PI10/743, PI13/414 grants and the *Miguel Servet* I3SNS and RETICS Programs (ISCIII).

References

1. Hsieh PC, Davis ME, Lisowski LK, Lee RT. Endothelial-cardiomyocyte interactions in cardiac development and repair. *Annu Rev Physiol* 2006;**68**:51–66.
2. Brutsaert DL. Cardiac endothelial-myocardial signaling: its role in cardiac growth, contractile performance, and rhythmicity. *Physiol Rev* 2003;**83**:59–115.
3. Brutsaert DL, Fransen P, Andries LJ, De Keulenaer GW, Sys SU. Cardiac endothelium and myocardial function. *Cardiovasc Res* 1998;**38**:281–290.
4. Brzezinska AK, Merkus D, Chilian WM. Metabolic communication from cardiac myocytes to vascular endothelial cells. *Am J Physiol Heart Circ Physiol* 2005;**288**:H2232–H2237.
5. Waldenstrom A, Genneback N, Hellman U, Ronquist G. Cardiomyocyte microvesicles contain DNA/RNA and convey biological messages to target cells. *PLoS ONE* 2012;**7**:e34653.
6. Deregibus MC, Cantaluppi V, Calogero R, Lo Iacono M, Tetta C, Biancone L, Bruno S, Bussolati B, Camussi G. Endothelial progenitor cell derived microvesicles activate an angiogenic program in endothelial cells by a horizontal transfer of mRNA. *Blood* 2007;**110**:2440–2448.
7. Janowska-Wieczorek A, Majka M, Kijowski J, Baj-Krzyworzeka M, Reca R, Turner AR, Ratajczak J, Emerson SG, Kowalska MA, Ratajczak MZ. Platelet-derived microparticles bind to hematopoietic stem/progenitor cells and enhance their engraftment. *Blood* 2001;**98**:3143–3149.
8. Andre F, Chaput N, Schartz NE, Flament C, Aubert N, Bernard J, Lemonnier F, Raposo G, Escudier B, Hsu DH, Tursz T, Amigorena S, Angevin E, Zitvogel L. Exosomes as potent cell-free peptide-based vaccine. I. Dendritic cell-derived exosomes transfer functional MHC class I/peptide complexes to dendritic cells. *J Immunol* 2004;**172**:2126–2136.
9. Garcia NA, González-King H, Ontoria I, Diez-Juan T, Sepuveda P. Glucose starvation in cardiomyocytes enhances exosome secretion and promotes angiogenesis in endothelial cells. *PLoS ONE* 2015;**10**:e0138849.
10. Sano S, Izumi Y, Yamaguchi T, Yamazaki T, Tanaka M, Shiota M, Osada-Oka M, Nakamura Y, Wei M, Wanibuchi H, Iwao H, Yoshiyama M. Lipid synthesis is promoted by hypoxic adipocyte-derived exosomes in 3T3-L1 cells. *Biochem Biophys Res Commun* 2014;**445**:327–333.
11. Ponnambalam S, Baldwin SA. Constitutive protein secretion from the trans-Golgi network to the plasma membrane. *Mol Membr Biol* 2003;**20**:129–139.
12. Savina A, Furlan M, Vidal M, Colombo MI. Exosome release is regulated by a calcium-dependent mechanism in K562 cells. *J Biol Chem* 2003;**278**:20083–20090.
13. Yu X, Harris SL, Levine AJ. The regulation of exosome secretion: a novel function of the p53 protein. *Cancer Res* 2006;**66**:4795–4801.
14. Barile L, Gherghiceanu M, Popescu LM, Moccetti T, Vassalli G. Ultrastructural evidence of exosome secretion by progenitor cells in adult mouse myocardium and adult human cardiospheres. *J Biomed Biotechnol* 2012;**2012**:354605.
15. Salomon C, Ryan J, Sobrevia L, Kobayashi M, Ashman K, Mitchell M, Rice GE. Exosomal signaling during hypoxia mediates microvascular endothelial cell migration and vasculogenesis. *PLoS ONE* 2013;**8**:e68451.
16. Lancaster GI, Febbraio MA. Mechanisms of stress-induced cellular HSP72 release: implications for exercise-induced increases in extracellular HSP72. *Exerc Immunol Rev* 2005;**11**:46–52.
17. Savina A, Vidal M, Colombo MI. The exosome pathway in K562 cells is regulated by Rab11. *J Cell Sci* 2002;**115**:2505–2515.
18. Kawauchi K, Araki K, Tobiume K, Tanaka N. p53 regulates glucose metabolism through an IKK-NF-kappaB pathway and inhibits cell transformation. *Nat Cell Biol* 2008;**10**:611–618.

19. Wood TE, Dalili S, Simpson CD, Hurren R, Mao X, Saiz FS, Gronda M, Eberhard Y, Minden MD, Bilan PJ, Klip A, Batey RA, Schimmer AD. A novel inhibitor of glucose uptake sensitizes cells to FAS-induced cell death. *Mol Cancer Ther* 2008;**7**:3546–3555.
20. Mittelbrunn M, Sanchez-Madrid F. Intercellular communication: diverse structures for exchange of genetic information. *Nat Rev Mol Cell Biol* 2012;**13**:328–335.
21. Fang Y, Vilella-Bach M, Bachmann R, Flanigan A, Chen J. Phosphatidic acid-mediated mitogenic activation of mTOR signaling. *Science* 2001;**294**:1942–1945.
22. Laulagnier K, Grand D, Dujardin A, Hamdi S, Vincent-Schneider H, Lankar D, Salles JP, Bonnerot C, Perret B, Record M. PLD2 is enriched on exosomes and its activity is correlated to the release of exosomes. *FEBS Lett* 2004;**572**:11–14.
23. Stenmark H. Rab GTPases as coordinators of vesicle traffic. *Nat Rev Mol Cell Biol* 2009; **10**:513–525.
24. Ostrowski M, Carmo NB, Krumeich S, Fanget I, Raposo G, Savina A, Moita CF, Schauer K, Hume AN, Freitas RP, Goud B, Benaroch P, Hacohen N, Fukuda M, Desnos C, Seabra MC, Darchen F, Amigorena S, Moita LF, Thery C. Rab27a and Rab27b control different steps of the exosome secretion pathway. *Nat Cell Biol* 2010;**12**:19–30.
25. Foster LJ, Weir ML, Lim DY, Liu Z, Trimble WS, Klip A. A functional role for VAP-33 in insulin-stimulated GLUT4 traffic. *Traffic* 2000;**1**:512–521.
26. Mittelbrunn M, Gutierrez-Vazquez C, Villarroya-Beltri C, Gonzalez S, Sanchez-Cabo F, Gonzalez MA, Bernad A, Sanchez-Madrid F. Unidirectional transfer of microRNA-loaded exosomes from T cells to antigen-presenting cells. *Nat Commun* 2011;**2**:282.
27. Yuyama K, Sun H, Mitsutake S, Igarashi Y. Sphingolipid-modulated exosome secretion promotes clearance of amyloid-beta by microglia. *J Biol Chem* 2012;**287**:10977–10989.
28. Ibrahim AG, Cheng K, Marban E. Exosomes as critical agents of cardiac regeneration triggered by cell therapy. *Stem Cell Rep* 2014;**2**:606–619.
29. Li J, Liu K, Liu Y, Xu Y, Zhang F, Yang H, Liu J, Pan T, Chen J, Wu M, Zhou X, Yuan Z. Exosomes mediate the cell-to-cell transmission of IFN-alpha-induced antiviral activity. *Nat Immunol* 2013;**14**:793–803.
30. Sahoo S, Klychko E, Thorne T, Misener S, Schultz KM, Millay M, Ito A, Liu T, Kamide C, Agrawal H, Perlman H, Qin G, Kishore R, Losordo DW. Exosomes from human CD34(+) stem cells mediate their proangiogenic paracrine activity. *Circ Res* 2011; **109**:724–728.
31. Parra-Bonilla G, Alvarez DF, Al-Mehdi AB, Alexeyev M, Stevens T. Critical role for lactate dehydrogenase A in aerobic glycolysis that sustains pulmonary microvascular endothelial cell proliferation. *Am J Physiol Lung Cell Mol Physiol* 2010;**299**: L513–L522.
32. Sluijter JP, Verhage V, Deddens J, van den Akker F, Doevendans PA. Microvesicles and exosomes for intracardiac communication. *Cardiovasc Res* 2014;**102**:302–311.
33. Subramani S, Malhotra V. Non-autophagic roles of autophagy-related proteins. *EMBO Rep* 2013;**14**:143–151.
34. Bodemann BO, Orvedahl A, Cheng T, Ram RR, Ou YH, Formstecher E, Maiti M, Hazelett CC, Wauson EM, Balakireva M, Camonis JH, Yeaman C, Levine B, White MA. RalB and the exocyst mediate the cellular starvation response by direct activation of autophagosome assembly. *Cell* 2011;**144**:253–267.
35. Geng J, Klionsky DJ. The Golgi as a potential membrane source for autophagy. *Autophagy* 2010;**6**:950–951.
36. Ghossoub R, Lembo F, Rubio A, Gaillard CB, Bouchet J, Vitale N, Slavik J, Machala M, Zimmermann P. Syntenin-ALIX exosome biogenesis and budding into multivesicular bodies are controlled by ARF6 and PLD2. *Nat Commun* 2014;**5**:3477.
37. Hirota Y, Kuronita T, Fujita H, Tanaka Y. A role for Rab5 activity in the biogenesis of endosomal and lysosomal compartments. *Biochem Biophys Res Commun* 2007;**364**: 40–47.
38. Rosenfeld JL, Moore RH, Zimmer KP, Alpizar-Foster E, Dai W, Zarka MN, Knoll BJ. Lysosome proteins are redistributed during expression of a GTP-hydrolysis-defective rab5a. *J Cell Sci* 2001;**114**:4499–4508.
39. Kypri E, Falkenstein K, De Lozanne A. Antagonistic control of lysosomal fusion by Rab14 and the Lyst-related protein LvsB. *Traffic* 2013;**14**:599–609.
40. Ao X, Zou L, Wu Y. Regulation of autophagy by the Rab GTPase network. *Cell Death Differ* 2014;**21**:348–358.
41. Sadacca LA, Bruno J, Wen J, Xiong W, McGraw TE. Specialized sorting of GLUT4 and its recruitment to the cell surface are independently regulated by distinct Rabs. *Mol Biol Cell* 2013;**24**:2544–2557.
42. Martin LB, Shewan A, Millar CA, Gould GW, James DE. Vesicle-associated membrane protein 2 plays a specific role in the insulin-dependent trafficking of the facilitative glucose transporter GLUT4 in 3T3-L1 adipocytes. *J Biol Chem* 1998;**273**:1444–1452.
43. Ferlito M, Fulton WB, Zauher MA, Marban E, Steenbergen C, Lowenstein CJ. VAMP-1, VAMP-2, and syntaxin-4 regulate ANP release from cardiac myocytes. *J Mol Cell Cardiol* 2010;**49**:791–800.
44. Jahn R, Scheller RH. SNAREs—engines for membrane fusion. *Nat Rev Mol Cell Biol* 2006; **7**:631–643.
45. Kluge MA, Fetterman JL, Vita JA. Mitochondria and endothelial function. *Circ Res* 2013; **112**:1171–1188.
46. Al-Nedawi K, Meehan B, Micallef J, Lhotak V, May L, Guha A, Rak J. Intercellular transfer of the oncogenic receptor EGFRvIII by microvesicles derived from tumour cells. *Nat Cell Biol* 2008;**10**:619–624.
47. Gross JC, Chaudhary V, Bartscherer K, Boutros M. Active Wnt proteins are secreted on exosomes. *Nat Cell Biol* 2012;**14**:1036–1045.
48. Sharghi-Namini S, Tan E, Ong LL, Ge R, Asada HH. Dll4-containing exosomes induce capillary sprout retraction in a 3D microenvironment. *Sci Rep* 2014;**4**:4031.
49. Sheldon H, Heikamp E, Turley H, Dragovic R, Thomas P, Oon CE, Leek R, Edelmann M, Kessler B, Sainson RC, Sargent I, Li JL, Harris AL. New mechanism for Notch signaling to endothelium at a distance by Delta-like 4 incorporation into exosomes. *Blood* 2010; **116**:2385–2394.
50. Divakaruni AS, Murphy AN. Cell biology. A mitochondrial mystery, solved. *Science* 2012;**337**:41–43.

Corrigendum

doi:10.1093/cvr/cvv278

Corrigendum to: Ilk conditional deletion in adult animals increases cyclic GMP-dependent vasorelaxation [Cardiovasc Res 2013; **99** (3): 535–544]

The authors wish to acknowledge the following funding information which was omitted from the above article: This work was supported by Health Institute Carlos III (PI1000612) cofunded with FEDER funds. The authors apologise for this omission.